Low core losses and soft magnetic properties of Fe-Al-Ga-P-C-B-Si glassy alloy ribbons with large thicknesses

doi: 10.1063/1.369803

Low core losses and soft magnetic properties of Fe–Al–Ga–P–C–B–Si glassy alloy ribbons with large thicknesses

Takao Mizushima,[a] Akihiro Makino, and Shoji Yoshida
Central Research Laboratory, Alps Electric Company, Limited, 1-3-5, Higashi-Takami, Nagaoka 940-8572, Japan

Akihisa Inoue
Institute for Materials Research, Tohoku University, 2-1-1, Katahira, Aoba-ku, Sendai 980-8577, Japan

The structure, soft magnetic properties, and core losses were investigated for a $Fe_{77}Al_{2.14}Ga_{0.86}P_{8.4}C_5B_4Si_{2.6}$ glassy alloy with a sheet thickness in a wide range from 30 to 240 μm prepared by the melt-spinning technique. The maximum thickness (t_{max}) for glass formation and the thermal stability (ΔT_x) of the supercooled liquid region defined by the difference between the crystallization temperature (T_x) and the glass transition temperature (T_g) are about 220 μm and 35 K, respectively. The saturation magnetization (σ_s) of this glassy alloy is about 1.5 T. The effective permeability at 1 kHz is as high as 12 000 in a thickness of 30 μm and it maintains high values above 4400 up to a thickness of t_{max}. The coercive force is kept at a low level, under 3 A/m up to t_{max}. This glassy alloy also shows low core loss values of 0.1–0.3 W/kg at $f=50$ Hz and $B_m=1.0$ T in the thickness from 30 to 220 μm. On the other hand, a $Fe_{78}Si_9B_{13}$ amorphous alloy shows almost the same low core losses as that of the glassy alloy only in a thickness of less than 70 μm. The difference between the dependence of the soft magnetic properties and the core loss on the thickness of these alloys should arise from their difference in ability of glass forming. The Fe–Al–Ga–P–C–B–Si glassy alloys should be very useful for inductive applications because of their thick ribbon shape and good soft magnetic properties in addition to low core loss. © *1999 American Institute of Physics.* [S0021-8979(99)37108-5]

I. INTRODUCTION

It has been known that the Fe-based amorphous alloy is a good core material for inductive applications because its core loss is much less than that of other metallic magnetic materials such as a silicon steel, etc. The shape of amorphous alloys, however, is usually limited to sheet, wire, and film because of the necessity of a high cooling rate resulting from their low glass-forming ability. For instance, the maximum thickness (t_{max}) to form a single amorphous phase of $Fe_{78}Si_9B_{13}$ amorphous ribbon is less than 100 μm. This limits its extension in some fields of application. It is pretty difficult to laminate thin amorphous ribbons to make transformers and/or inductors and also to improve the lamination factor. Consequently, the bulky amorphous alloys are desirable from the point of view of application.[1]

Recently bulk amorphous alloys have been formed in multicomponent Mg-, Ln-, (Ln=lanthanoide metal) Zr-, and Zr–Ti-based alloy systems.[2–7] These bulk amorphous alloys have a wide more than 60 K supercooled liquid region before crystallization. The appearance of the wide supercooled liquid region implies a high resistance against crystallization, leading to a better glass-forming ability. The above-mentioned bulk amorphous alloys invariably satisfy the following three empirical rules for achieving large glass-forming ability: (1) multicomponent alloy systems consisting of more than three elements, (2) significantly different atomic size ratios above about 12% among the main constituent elements, and (3) negative heats of mixing among their elements. Following these empirical rules, we subsequently searched for a new Fe-based amorphous alloy with high glass-forming ability. We have already reported that a $Fe_{72}Al_{2.14}Ga_{0.86}P_{9.65}C_{5.75}B_{4.6}Si_{2.6}$ amorphous alloy sheet has a wide supercooled liquid region exceeding 60 K before crystallization and maximum thickness (t_{max}) for glass forming of 190 μm.[8] We have tried to further investigate the relation between the glass-forming ability and soft magnetic properties for this glassy alloy system.

This article is intended to present the thermal stability of the supercooled liquid region and soft magnetic properties of a Fe–Al–Ga–P–C–B–Si glassy alloy prepared by the melt-spinning method. In addition, the dependence of core loss on sample thickness for these glassy alloys is also reported.

II. EXPERIMENTAL PROCEDURE

A multicomponent $Fe_{77}Al_{2.14}Ga_{0.86}P_{8.4}C_5B_4Si_{2.6}$ alloy was used in this study because of its wide supercooled liquid region before crystallization and very high saturation magnetization (σ_s) in the Fe–Al–Ga–P–C–B–Si system.[9] Its alloy ingots were prepared by induction melting mixtures of pure Fe, Al, Si, and Ga metals, premelted Fe–P and Fe–C alloys, and pure crystal boron in an argon atmosphere. Rapidly solidified alloy ribbons 1 mm in width and various thickness ranging from 30 to 240 μm were prepared through control of the wheel velocity and the diameter of the slot of the nozzle, and by ejection pressure by a single roller melt-spinning method. The amorphous nature was examined by x-ray diffraction (XRD) and optical and transmission elec-

[a]Electronic mail: mizushim@alps.co.jp

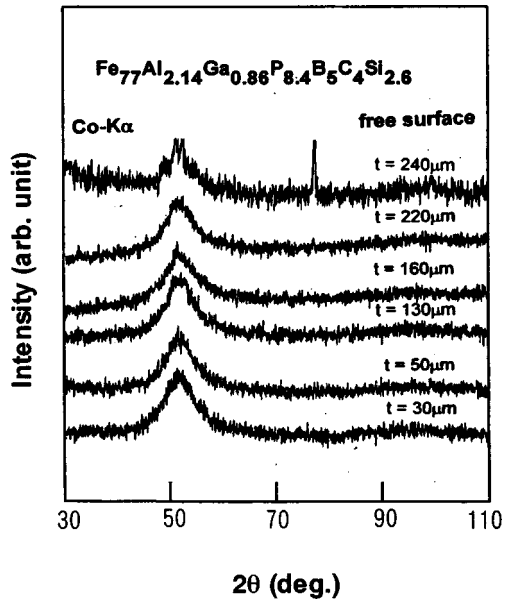

FIG. 1. XRD patterns taken from the freely solidified surface in the melt-spun $Fe_{77}Al_{2.14}Ga_{0.86}P_{8.4}C_5B_4Si_{2.6}$ with various thicknesses ranging from 30 to 240 μm.

tron microscopies (OM and TEM). The thermal stability associated with a glass transition, supercooled liquid region and crystallization was examined at a heating rate of 0.67 K/s by differential scanning calorimetry (DSC). The saturation magnetization (σ_s), coercive force (H_c), permeability (μ_e) at 1 kHz, and core loss were measured at room temperature with a vibrating sample magnetometer (VSM) under 800 kA/m, a $B-H$ loop tracer under 1.6 kA/m, an impedance analyzer under 0.8 A/m, and a single sheet tester (SST), respectively.

III. RESULTS

A. Structure and thermal stability

Figure 1 shows the XRD patterns taken from the freely solidified surface of the melt-spun ribbons with thicknesses ranging from 30 to 240 μm. The samples with thicknesses below 220 μm consist only of a broad peak at a wave vector ($K_p = 4\pi \sin\theta/\lambda$) of about 31 nm^{-1}. But, a further increase in thickness up to 240 μm causes the formation of coexisting amorphous and Fe_3B phases. It is concluded, therefore, that the critical sample thickness for glass formation by the conventional melt spinning method lies around 220 μm, which is much larger than that (=70–100 μm) of Fe–Si–B amorphous alloys.

Figure 2 shows the DSC curves of melt-spun $Fe_{77}Al_{2.14}Ga_{0.86}P_{8.4}C_5B_4Si_{2.6}$ alloys with thicknesses of 30, 130, 220, and 240 μm. Although the glass transition temperature (T_g) remains constant in the entire thickness range, the onset temperature of crystallization (T_x) keeps a constant value in the thickness range up to 220 μm and decreases slightly for 240 μm. However, no appreciable change in the two stage exothermic peak behavior is observed, indicating that the 220 μm thick sheet consists mainly of an amorphous phase. The small endothermic peak marked by the arrow is

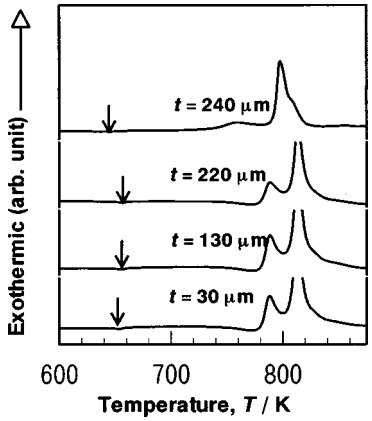

FIG. 2. DSC curves of the melt-spun $Fe_{77}Al_{2.14}Ga_{0.86}P_{8.4}C_5B_4Si_{2.6}$ with thicknesses of 30, 130, 220, and 240 μm. The arrows indicate the Curie temperature (T_c).

due to the transition from ferromagnetism to paramagnetism. There is a tendency for the Curie temperature (T_c) to increase with an increase in sample thickness due to its structural relaxation.[10]

B. Magnetic properties and core loss

Figure 3 shows the dependence of σ_s, H_c, and μ_e on sample thickness for a $Fe_{77}Al_{2.14}Ga_{0.86}P_{8.4}C_5B_4Si_{2.6}$ glassy alloy and a $Fe_{78}Si_9B_{13}$ amorphous ribbon. The values of σ_s and H_c for each sample with an amorphous state do not depend on their thickness. The σ_s for the Fe-based glassy alloy is slightly smaller than that of the $Fe_{78}Si_9B_{13}$ amor-

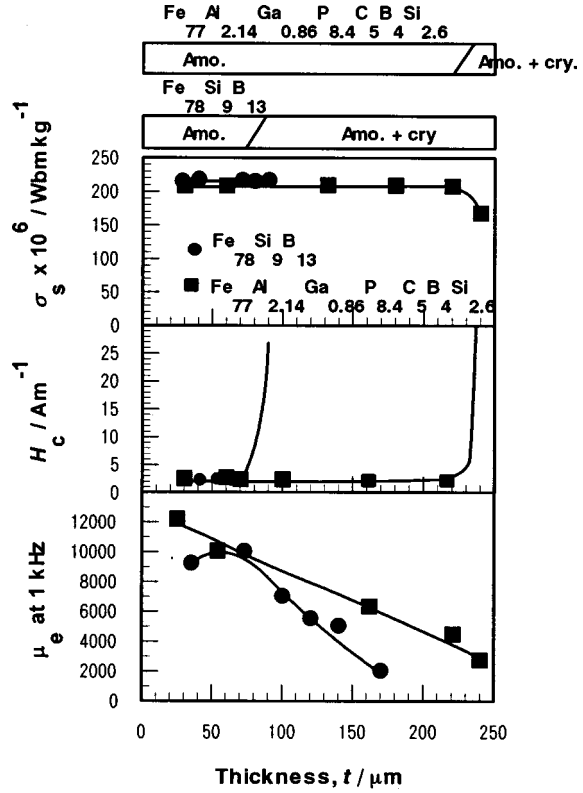

FIG. 3. Changes in σ_s, H_c, and μ_e for the $Fe_{77}Al_{2.14}Ga_{0.86}P_{8.4}C_5B_4Si_{2.6}$ glassy alloy and the $Fe_{78}Si_9B_{13}$ amorphous ribbon as a function of sample thickness.

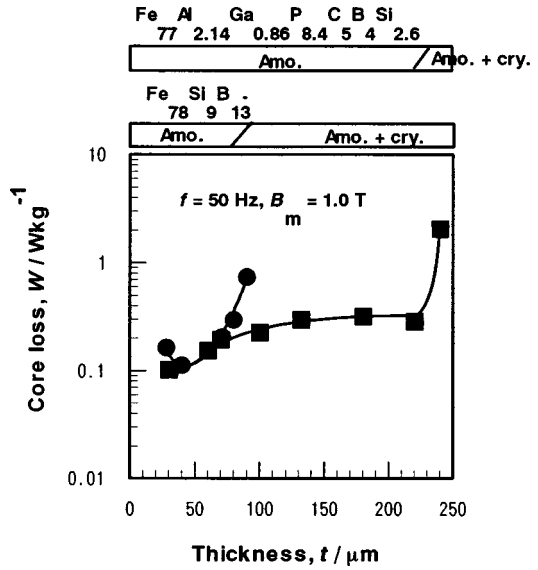

FIG. 4. Changes in core losses at $f=50$ Hz and $B_m=1.0$ T for the $Fe_{77}Al_{2.14}Ga_{0.86}P_{8.4}C_5B_4Si_{2.6}$ glassy alloy and the $Fe_{78}Si_9B_{13}$ amorphous ribbon as a function of sample thickness. The structures of both samples confirmed by XRD are also shown.

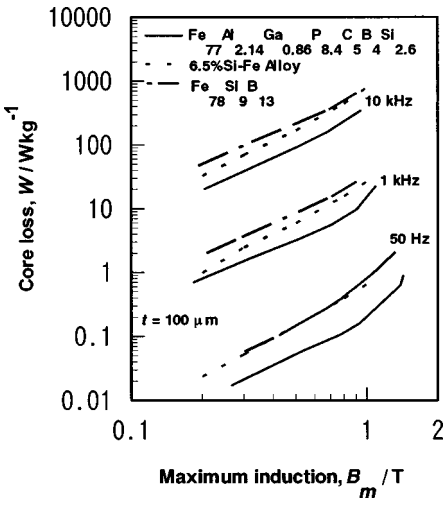

FIG. 5. Changes in core losses for the $Fe_{77}Al_{2.14}Ga_{0.86}P_{8.4}C_5B_4Si_{2.6}$ glassy alloy, 6.5% Si–Fe, and the $Fe_{78}Si_9B_{13}$ amorphous ribbon with sample thickness of 100 μm at $f=50$ Hz, 1 kHz, and 10 kHz as a function of B_m.

phous ribbon. The H_c for each sample shows the same value of about 3 A/m under t_{max} and becomes larger over each t_{max}. Because the t_{max} of the Fe-based glassy alloy is larger than that of the $Fe_{78}Si_9B_{13}$ amorphous ribbon, a small H_c remains at the wide sample thickness range for the Fe-based glassy alloy. The μ_e for the $Fe_{77}Al_{2.14}Ga_{0.86}P_{8.4}C_5B_4Si_{2.6}$ glassy alloy decreases gradually with an increase in sample thickness. The μ_e for the Fe-based glassy alloy, however, is larger than that for the Fe–Si–B amorphous ribbon in the whole thickness range.

Figure 4 shows the change in the core loss at a frequency of 50 Hz and a maximum flux density (B_m) of 1.0 T for the $Fe_{77}Al_{2.14}Ga_{0.86}P_{8.4}C_5B_4Si_{2.6}$ glassy alloy and the $Fe_{78}Si_9B_{13}$ amorphous ribbon as a function of sample thickness. The core loss for the Fe-based glassy alloy increases slightly with an increase in sample thickness, and thereafter becomes a remarkably large value above t_{max}. On the other hand, the core loss for the Fe–Si–B amorphous alloy reaches a minimum at a sample thickness of about 50 μm, whereas it increases dramatically with an increase in sample thickness. The increase in core losses for both samples over each t_{max} should be the result of precipitation of the crystalline phase.[11] The Fe-based glassy alloy shows a lower core loss than the Fe–Si–B alloy in the whole thickness range mainly due to its higher glass-forming ability.

The dependence of the core loss of the $Fe_{77}Al_{2.14}Ga_{0.86}P_{8.4}C_5B_4Si_{2.6}$ glassy alloy with a sample thickness of 100 μm at $f=50$ Hz, 1 kHz, and 10 kHz on B_m is shown in Fig. 5. The dependence of the core loss of the 6.5% Si–Fe alloy and the $Fe_{78}Si_9B_{13}$ amorphous ribbon in the same sample thickness are also shown for the purpose of comparison. The core loss for the Fe–Al–Ga–P–C–B–Si glassy alloy is much lower than that of the 6.5% Si–Fe alloy and the Fe–Si–B amorphous ribbon for the whole range of B_m at each frequency because of its good soft magnetic properties, shown in Fig. 3, and high electrical resistivity. The electrical resistivity for the Fe–Al–Ga–P–C–B–Si glassy alloy is $160\times10^{-8}\,\Omega$ m, which is higher than the $82\times10^{-8}\,\Omega$ m for the 6.5% Si–Fe alloy, and $137\times10^{-8}\,\Omega$ m for the Fe–Si–B alloy.

The Fe–Al–Ga–P–C–B–Si glassy alloy should be useful as an engineering material because of its great glass-forming ability as well as for its low core loss and excellent soft magnetic properties.

ACKNOWLEDGMENT

This work was supported by the New Energy and Industrial Technology Development Organization (NEDO) through the R&D Institute of Metals and Composites for Future Industries (RIMCOF).

[1] E. Matsubara, T. Yamamura, T. Waseda, A. Inoue, T. Zhang, and T. Masumoto, Mater. Trans., JIM **33**, 873 (1992).
[2] A. Inoue, T. Zhang, and T. Masumoto, Mater. Trans., JIM **30**, 965 (1989).
[3] A. Inoue, K. Ohtera, K. Kita, and T. Masumoto, Jpn. J. Appl. Phys., Part 2 **27**, L2284 (1988).
[4] A. Inoue, T. Zhang, and T. Masumoto, Mater. Trans., JIM **31**, 177 (1990).
[5] A. Inoue, N. Nishiyama, N. Amiya, T. Zhang, and T. Masumoto, Mater. Lett. **19**, 131 (1994).
[6] A. Amiya, N. Nishiyama, A. Inoue, and T. Masumoto, Mater. Sci. Eng., A **179/180**, 692 (1994).
[7] A. Peker and W. L. Johnson, Appl. Phys. Lett. **63**, 2324 (1993).
[8] T. Mizushima, A. Makino, and A. Inoue, IEEE Trans. Magn. **33**, 3784 (1997).
[9] T. Mizushima, A. Makino, and A. Inoue, J. Appl. Phys. **83**, 6329 (1998).
[10] H. S. Chen, Rep. Prog. Phys. **43**, 353 (1980).
[11] H. N. Ok and H. Morrish, J. Appl. Phys. **52**, 1835 (1981).